THE RESONANCE CONES OF ELECTRON PLASMA WAVES IN TOROIDAL, INHOMOGENEOUS PLASMAS

P. Javel, G. Müller and U. Weber
Max-Planck-Institut für Plasmaphysik, Garching b. München

and

R.R. Weynants
Laboratorium voor Plasmafysica, Associatie EURATOM-Belgische Staat, Koninklijke Militaire School, 1040 Brussels

IPP 2/228 March 1975

MAX-PLANCK-INSTITUT FÜR PLASMAPHYSIK

GARCHING BEI MÜNCHEN

MAX-PLANCK-INSTITUT FÜR PLASMAPHYSIK

GARCHING BEI MÜNCHEN

THE RESONANCE CONES OF ELECTRON PLASMA WAVES IN TOROIDAL, INHOMOGENEOUS PLASMAS

P. Javel, G. Müller and U. Weber
Max-Planck-Institut für Plasmaphysik, Garching b. München

and

R. R. Weynants
Laboratorium voor Plasmafysica, Associatie EURATOM-Belgische Staat, Koninklijke Militaire School, 1040 Brussels

IPP 2/228 March 1975

Die nachstehende Arbeit wurde im Rahmen des Vertrages zwischen dem Max-Planck-Institut für Plasmaphysik und der Europäischen Atomgemeinschaft über die Zusammenarbeit auf dem Gebiete der Plasmaphysik durchgeführt.

THE RESONANCE CONES OF ELECTRON PLASMA WAVES IN TOROIDAL, INHOMOGENEOUS PLASMAS

P. Javel, G. Müller and U. Weber
Max-Planck-Institut für Plasmaphysik, Garching b. München

and

R. R. Weynants
Laboratorium voor Plasmafysica, Associatie EURATOM-Belgische Staat, Koninklijke Militaire School, 1040 Brussels

IPP 2/228

Abstract

The resonance cones of electron plasma waves, their trajectory and the related wave dispersion are observed and confirmed under the combined influence of toroidicity, strong inhomogeneity and energy depletion by ionization and heating up to close to the lower hybrid density. The fine structure within the cone typical for finite length exciters is also verified.

The Resonance Cones of Electron Plasma Waves in Toroidal, Inhomogeneous Plasmas

It is well known that radio frequency energy can be carried towards the lower hybrid layer by means of electron plasma waves. The cold-plasma dispersion of these waves under the conditions studied here ($\omega_{ci}^2 \ll \omega^2 \ll \omega_{ce}^2$ and $\omega \ll k_z c$) is given by

$$k_\perp^2 = k_z^2 \frac{(\omega_{pe}^2 - \omega^2)}{(\omega^2 - \omega_{LH}^2)\left(1 + \frac{\omega_{pe}^2}{\omega_{ce}^2}\right)} \qquad (1)$$

where ω is the wave frequency, ω_{pe} and ω_{pi} are the electron and ion plasma frequencies, ω_{ce} and ω_{ci} are the electron and ion cyclotron frequencies. The lower hybrid frequency is $\omega_{LH} = \omega_{pi}\left(1 + \frac{\omega_{pe}^2}{\omega_{ce}^2}\right)^{-1/2}$ when $\omega_{pi}^2 \gg \omega_{ci}^2$ and $k_\perp$ and k_z are the wavenumbers perpendicular and parallel to the magnetic field respectively. As the differential equation for the wave amplitude is of the hyperbolic type, the energy emanating from a finite rf source is localized along well-defined surfaces, called resonance cones (FISHER and GOULD, 1971; KUEHL, 1973), which make an approximate angle with the magnetic axis

$$\psi = \tan^{-1}\left[(\omega^2 - \omega_{LH}^2)\left(1 + \frac{\omega_{pe}^2}{\omega_{ce}^2}\right) \Big/ (\omega_{pe}^2 - \omega^2)\right]^{1/2} . \qquad (2)$$

Recently, BELLAN and PORKOLAB (1974) published some computations concerning the detailed wave pattern within the resonance cones propagating from a finite length parallel plate source into an inhomogeneous plasma slab. They calculate the potential distribution inside the plasma for a potential $\phi = \phi_o e^{-i\omega t}$ applied to the plates and find that an essential role is played by the cones (i.e. characteristics of the differential equation) emanating from the ends of the plates. Indeed, they find a real part of the potential which is only different from zero between the two trajectories mentioned above and which is then essentially an image of the potential distribution at the plates. Furthermore, they compute an imaginary part which consists of logarithmic singularities along the same trajectories. Both real and imaginary parts are weighted by the same

density dependent factor. In the following, the term "cone" will be used for the complete wave pattern including edge effects. In their most recent publication BELLAN and PORKOLAB (1975) reported experimental evidence for their predictions in cylindcrical geometry using a multiple-ring coupling structure.

Here, we report experimental confirmation of the resonance cone-propagation properties and of its detailed wave structure in toroidal geometry under the interesting condition that the electron plasma waves sustain the plasma in which they propagate self-consistently. As a result, the resonance cone properties are verified even when the waves strongly interact with the plasma through both ionization and plasma heating. In the present paper, we restrict ourselves to the purely kinematic aspects of the waves whereas the concomitant heating processes will be in detail discussed elsewhere (JAVEL et al., 1975).

The experiments are performed on the Wendelstein stellarator W II a, having a major radius R = 50 cm and a maximum minor radius a = 6 cm; the toroidal field B_o is varied up to 6 kG and the rotational transform ι is mostly in the range 0 to 0.2. The working gas is hydrogen at pressures of about 10^{-5} Torr. The radio frequency power is coupled into the machine via one or two electrostatic ring-shaped electrodes of 10cm diameter and 4cm length which at the same time serve as limiter. The applied power $P = P_{inc} - P_{refl}$, which creates the plasma and is propagated along the machine via the electron waves is up to 300 W cw in the frequency range 35 to 200 MHz. Maximum plasma densities of 7×10^{11} cm^{-3} are thus attained. The electron temperature is typically $T_e \leq 15$eV. Ion Temperatures up to 5 eV are measured by an electrostatic analyser in the plasma edge region. The waves are detected by means of radially movable coaxial rf probes and analyzed by means of a vector voltmeter where the pick-up signal is compared in amplitude and phase with the driver signal.

Fig. 2a shows a typical sequence of radial plasma density profiles for f = 50 MHz and various power levels. These curves represent the ion-saturation current to a small Langmuir probe while the absolute density values are checked by means of 4mm interferometry. When comparing the curves at 15W and 95W, one can see that

the density level is about the same and that only a broadening of the profile occurs with increasing power. This behaviour is characteristic for this type of plasma production (BERNABEI et al., 1974), where the value of the peak density is observed to be the density for which the corresponding lower hybrid frequency (here $\omega_{LH} \approx \omega_{pi}$) approaches the applied frequency. This feature in itself is the most direct proof of the sustainment of the plasma by means of electron plasma waves which indeed can only exist for densities such that $\omega_{LH} < \omega$ (see Eq.1). Due to the observed strong radial variation of the electron and ion temperatures, which furthermore can be comparable in magnitude, the interpretation of the ion-saturation current is subjected to uncertainties. It is,therefore, impossible to ascertain how closely the lower hybrid density can be approached, or whether it even could be exceeded , as it sometimes has the appearance.

Figure 2b, showing the radial rf potential distribution measured at an axial distance from the source of 53cm, exhibits the expected resonant behaviour. The conical surface leaving the coupling structure is intersected twice by the probe and two distinct potential maxima are recorded. As seen in Fig. 2c, the signal phase also changes markedly when the cone is crossed. The radial position to which the cone has progressed follows the predictions of Eq. (2), i.e. when the density (read power) is lowered, the angle ψ steepens and the cone shifts radially inwards at a fixed probe position. This is further corroborated in Fig.3, where we plot, as a function of rf power and for different frequencies, the radial displacements with respect to the launching structure of the two cone-intersections. The lines give the corresponding positions as found from a graphical integration of Eq. (2) from the position of the rf structure up to the observation plane using the particular density profile pertaining to each experimental condition. The agreement between theory and experiment is quite satisfactory, in particular when one considers the sometimes rather steep density gradients.

We now proceed to compare the rf potential measurements with the theory, put forward by BELLAN and PORKOLAB (1974). In Fig.4a and 4b we give a schematic

extrapolation of these theoretical predictions under conditions corresponding to our experimental situation. As one should be able to discriminate between real and imaginary parts and as only the relative phase difference between the probe signal and the driving signal is measured, we construct a polar diagram and choose that absolute initial phase which provides the best fit with theory. Fig. 5a shows the result of such a procedure for the excitation by one electrode and proves that it is indeed possible to resolve the rf potential into a real and imaginary part with the anticipated characteristics (Fig. 4a). The equivalent of the theoretical logarithmic singularities leaving the ends of the couplers are well defined maxima which are located in the region of steepest Re ϕ gradients. The smearing out of both real and imaginary parts is not surprising and has been discussed by BELLAN et al. (1974). In Fig. 5b the rf power has been lowered resulting in a decreased plasma density. Now, the measuring probe intersects the conical resonance surface beyond the vertex, as schematized in Fig. 4a, case II. On penetration into the plasma, the probe, therefore, first meets the pattern emanating from the coupler inside, a fact which is clearly evident in the imaginary ϕ part. One should also note the inverted rotation sense of the polar diagram.

In Fig. 6 we show a typical result for an excitation by means of two identical couplers fed in phase opposition (Fig. 4b). One notes that the real part of the potential once more reflects the applied potential distribution at the source. The imaginary part on the other hand reveals a maximum whenever the slope of the real part changes sign. Here again the theoretical decomposition schematically reflected in Fig. 4b seems to be fully warranted. Between the cones, i.e. around the axis, the polar curve reveals a fine structure which is not accounted for yet. When driving the two couplers in phase, we do not find an essential difference with the results of one structure. The phase opposition measurements in principle also allow a direct verification of the dispersion relation Eq. (1). The exciting structure imposes a k_z spectrum with a peak distribution around $k_z = \frac{2\pi}{2o}\,cm^{-1}$ corresponding to twice the structure length. This k_z will be dominant along the entire cone-trajectory. Furthermore, the number of applied axial periods should be retrieved as an equal number of radial periods. In Fig. 6 one finds that for the cone intersection to the left

$\lambda_\perp/2 = \pi/k_\perp$ (180 degrees in phase change) amounts to 10mm and for the right one to 4mm. According to Eq. (1) and the measured densities at the average cone location (with the reservation expressed previously), these figures should be about 3mm and 0mm. The discrepancy between theory and experiment is usually of the above order of magnitude and goes in the same sense. While one expects that the finite length of the probe tips (1.5mm) leads to a smearing out of the phase change, this effect only does not suffice to explain the difference.

Nevertheless, we believe that the combined results on cone position and radial wavelength confirm the dispersion relation under conditions which have not been studied before to our knowledge, i.e. strong inhomogeneity, toroidicity and small $\frac{\omega - \omega_{LH}}{\omega_{LH}}$ ratios.

At this point, it is appropriate to discuss two further experimental observations:

(i) The existence of the resonance cone which confines the rf energy over a narrow radial range clearly enhances the possible occurrence of parametric decay, as the appropriate threshold fields can more easily be achieved than would be the case for a more uniform distribution mechanism. Under our experimental conditions we observe for power levels as low as 10 W parametric instability involving an electron plasma sideband-wave and a low frequency ion wave with frequency close to the ion-cyclotron frequency. As the sideband wave has a frequency which is only slightly different from the pump frequency, the sideband wave also follows a conical trajectory which practically coincides with that of the pump. Even the energy density of the ion wave appears to be highly localized as the radial field distribution is roughly proportional to that of the sideband wave, a result which might be interpreted in terms of the Manley-Rowe relation (see e.g. PORKOLAB, 1974). Under those circumstances, it is clear that the occurrence of the resonance wave is not an isolated kinematic event: the plasma production and the heating of both electrons (via the sideband wave) and ions (via the ion wave) will be marked by this strong energy localization. These important aspects will be discussed in a forthcoming paper (JAVEL et al., 1975).

(ii) We find that the fine structure of the fields within the resonance cone does not have a marked effect on the plasma production capability, as seen e.g. from a comparison between the density profiles of Fig.2 with that of Fig.5 related to the double structure. As far as heating is concerned, especially ion heating, one might expect more pronounced effects, as the distribution within the cone could be "tuned", via the distribution at the source and via the decay selection rules, to a k_z which would be particularly favourable for ion-cyclotron damping. This aspect is under further experimental study.

Acknowledgement

The authors are indebted to Dr.A.v.H.van Oordt for cooperation in the starting phase of experiments and diagnostics and they wish to acknowledge the technical assistance of G.Abele, P.Böhm, K.-H.Brumm, R.Dunkel, A.Gronmayer, D.Köhler, F.Leitl, and W.Spensberger in preparations of the experiments and in operating the machine.

References

1) BELLAN P. and PORKOLAB M., Phys. Fluids 17, 1592 (1974).

2) BELLAN P. and PORKOLAB M., Phys. Rev. Lett. 34, 124 (1975).

3) BERNABEI S., HOOKE W.M., JASSBY D.L., and MOTLEY R.W., Proceedings of the Second Topical Conference on rf Plasma Heating, Lubbock, Texas (1974), paper C 5 .

4) FISHER R.K. and GOULD R.W., Phys. Fluids 14, 857 (1971).

5) JAVEL et al., to be published.

6) KUEHL H.H., Phys. Fluids 16, 1311 (1973).

7) PORKOLAB M., Proceedings of the Second Topical Conference on rf Plasma Heating, Lubbock, Texas (1974), paper D 1.

Figure Captions

1. Experimental set-up showing the general diagnostic instruments.

2. Typical radial profiles of density (a), rf amplitude (b) and rf phase (c). The applied frequency is 50 MHz, B_o = 5 kG, t = 0.11, p = 3.5 10^{-5} Torr. The rf measurements are performed at 53 cm from the source.

3. Radial displacement with respect to the launching structure of both cone intersections (a and b) as a function of rf power P. The experimental points pertain to frequencies of 50 MHz (●), 85 MHz (△) and 110 MHz (■). The excitation occurs by means of two electrodes and the observation plane is situated at 58 cm from the coupler midplane. The lines give the expected cone positions as found from integration of Eq. (2).

4.(a) Schematical wave pattern emanating from a ring-shaped coupler and expected potential distribution as picked up by probes intersecting the conical surface on either side of the vertex. Also sketched is the density profile.

(b) Idem for wave pattern produced by two identical couplers driven in phase opposition. The dotted lines represent the expected smearing out.

5.(a) Density profile (N), polar diagram of rf potential and its radially resolved real (Re ϕ) and imaginary (Im ϕ) parts. f = 85 MHz, P = 22 W, B_o = 5 kG, t = 0.11, p = 3.5 10^{-5} Torr. The rf measurements are performed at 53 cm from the source. The graduation on the polar curves marks the radial probe position every half a centimeter.

(b) Corresponding results for P = 12 W.

6. Density profile, polar diagram of rf potential and its radially resolved real and imaginary parts for an excitation by means of two ring-shaped couplers driven in phase opposition. The rf observation port is located at 58cm from the midplane of the double structure. P = 36 Watt, f = 50 MHz, B_o = 5 kG, t = 0.11, p = 3.5 10^{-5} Torr.

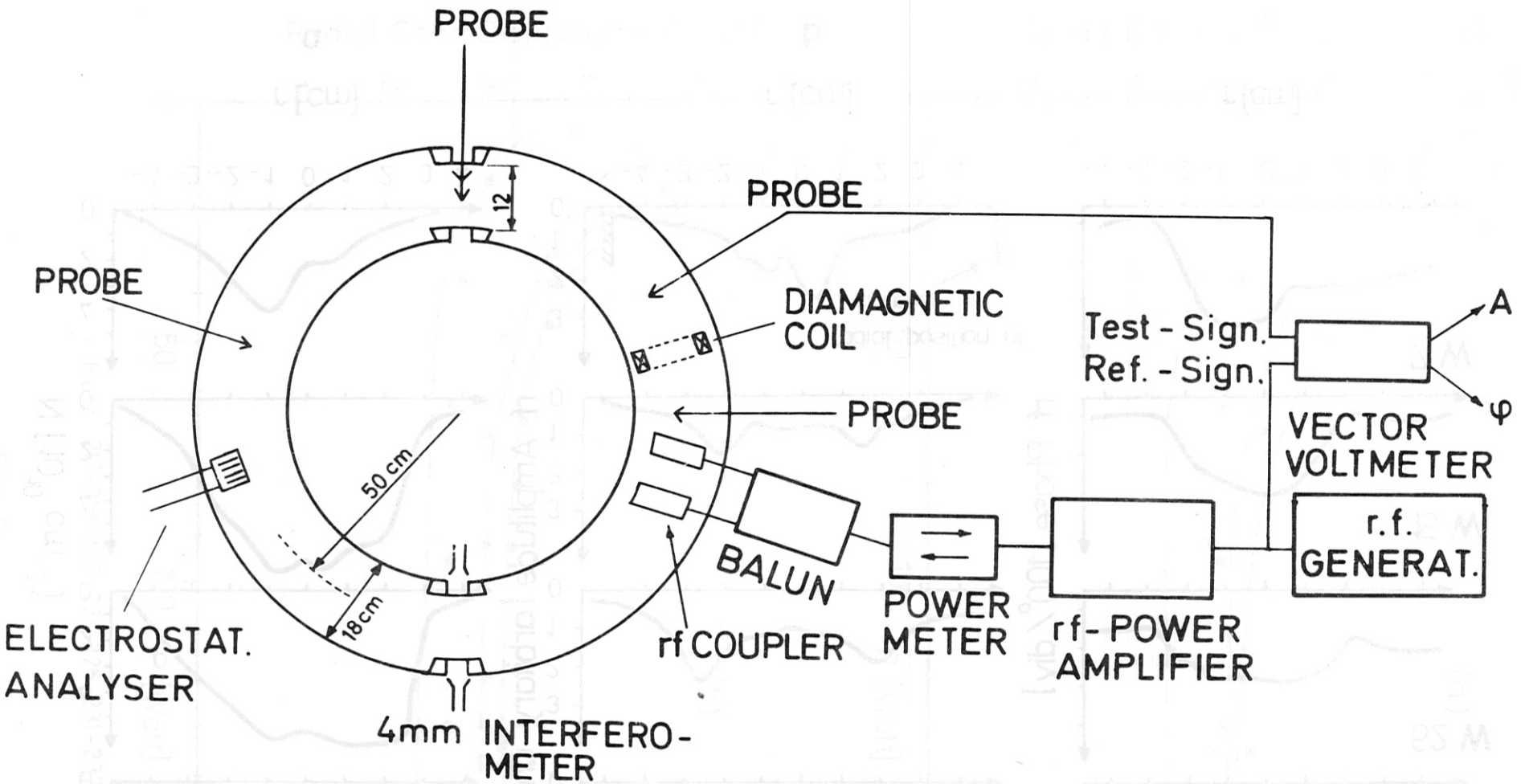
PROBE
PROBE
PROBE
PROBE
12
DIAMAGNETIC
COIL
Test - Sign.
Ref. - Sign.
A
φ
VECTOR
VOLTMETER
50 cm
18cm
BALUN
POWER
METER
rf - POWER
AMPLIFIER
r.f.
GENERAT.
ELECTROSTAT.
ANALYSER
rf COUPLER
4mm INTERFERO-
METER

Fig.1

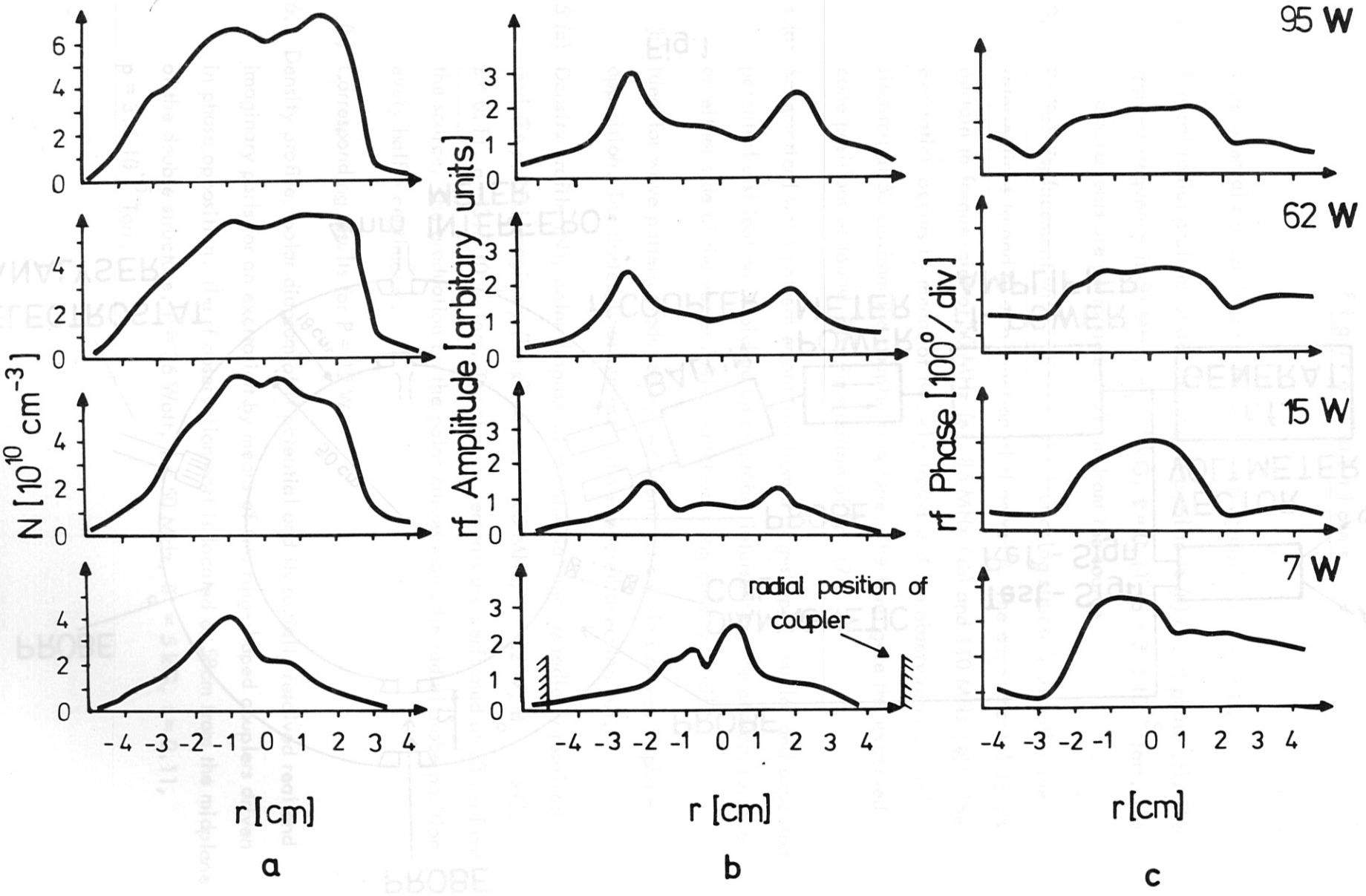
95 W
62 W
15 W
7 W
N [10^10 cm^-3]
rf Amplitude [arbitary units]
rf Phase [100°/div]
radial position of coupler
r [cm]
r [cm]
r [cm]
a
b
c

Fig. 2

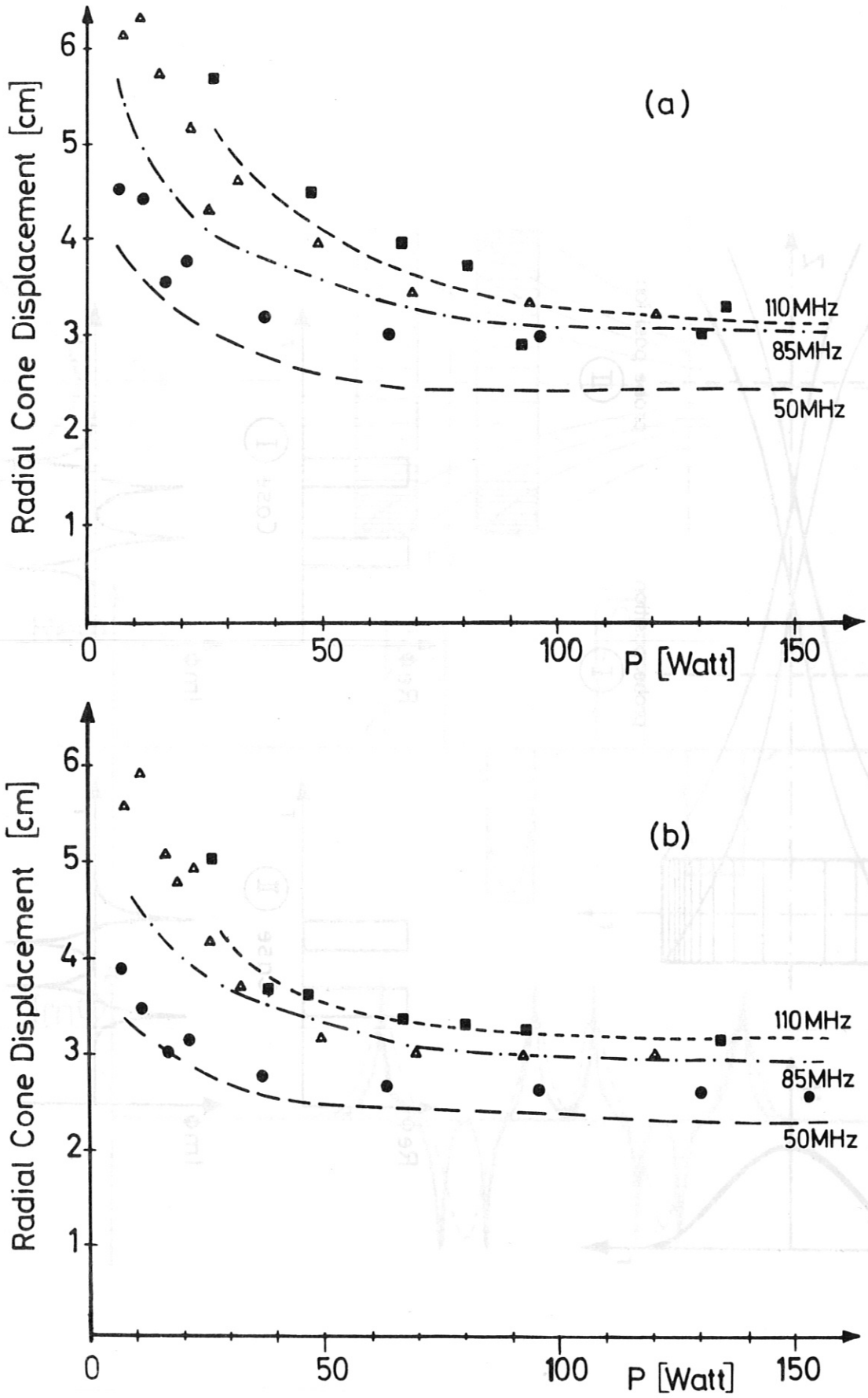

Runs 217-218-220-224-226-231-237

Fig. 3

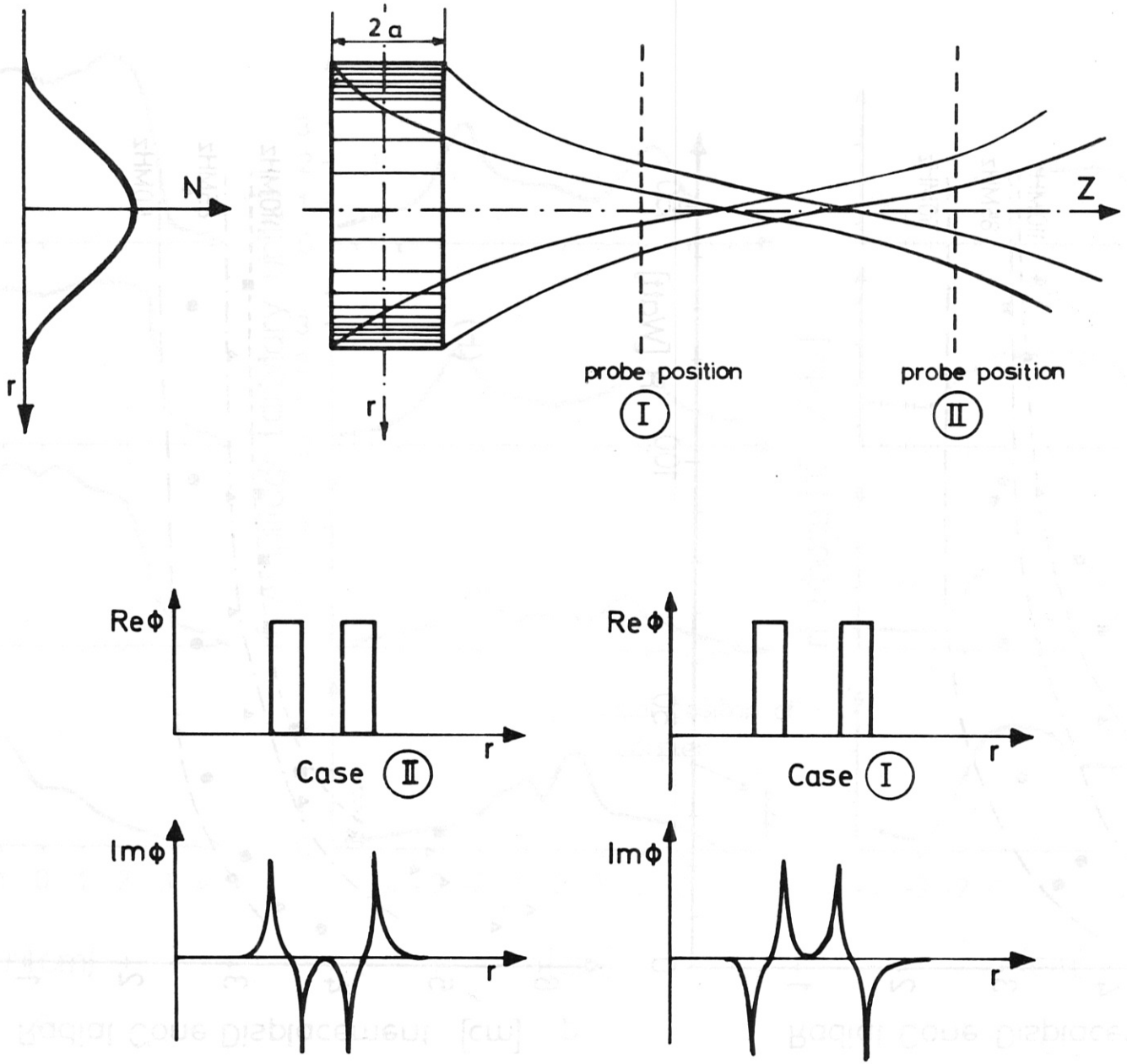
N
r
2a
r
Z
probe position
I
probe position
II
Reϕ
r
Case II
Reϕ
r
Case I
Imϕ
r
Imϕ
r

Fig. 4a

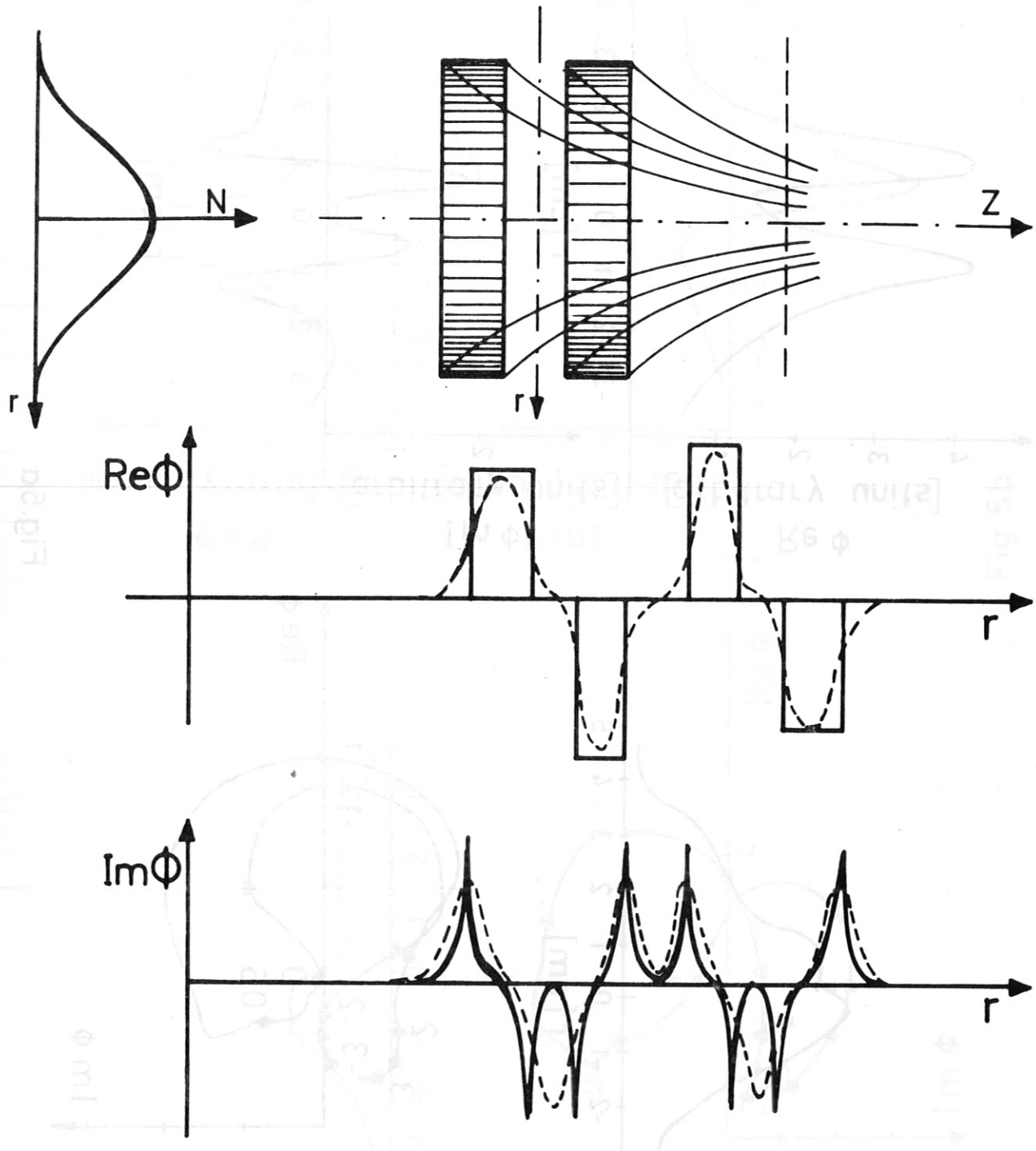

Fig. 4b

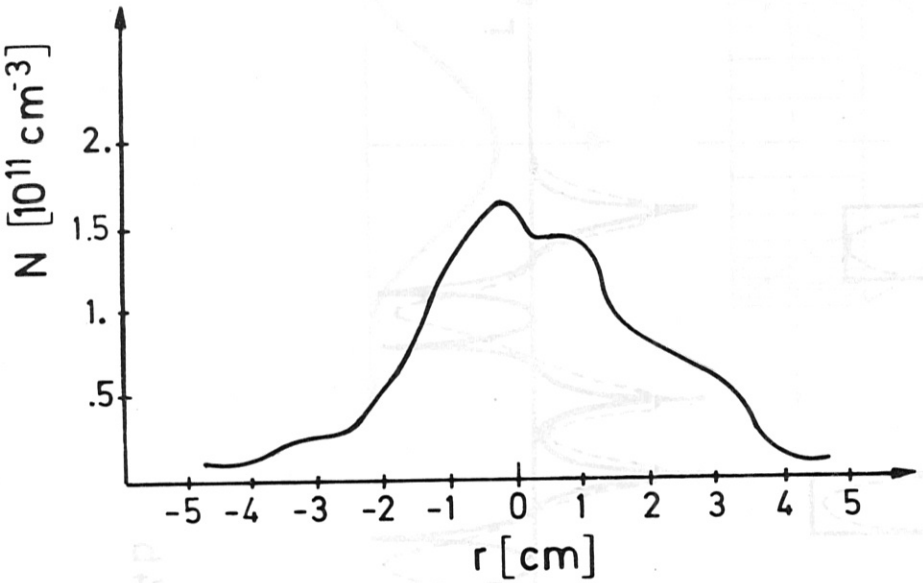
N [10^11 cm^-3]
2.
1.5
1.
.5
-5 -4 -3 -2 -1 0 1 2 3 4 5
r [cm]

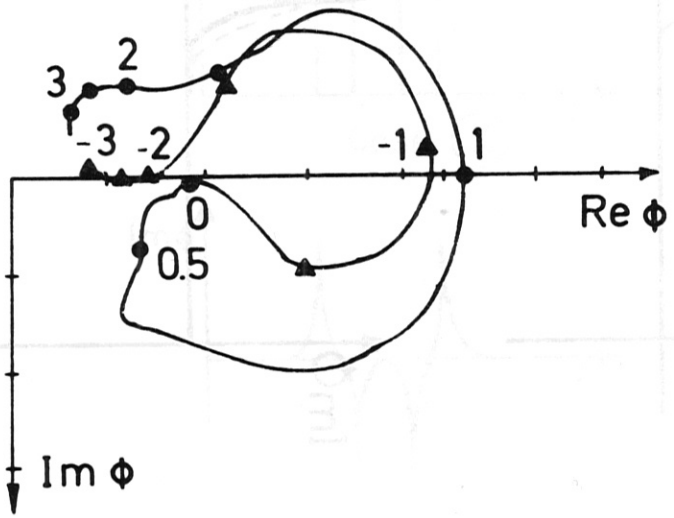
3
2
1
-3
-2
-1
1
0
0.5
Re φ
Im φ

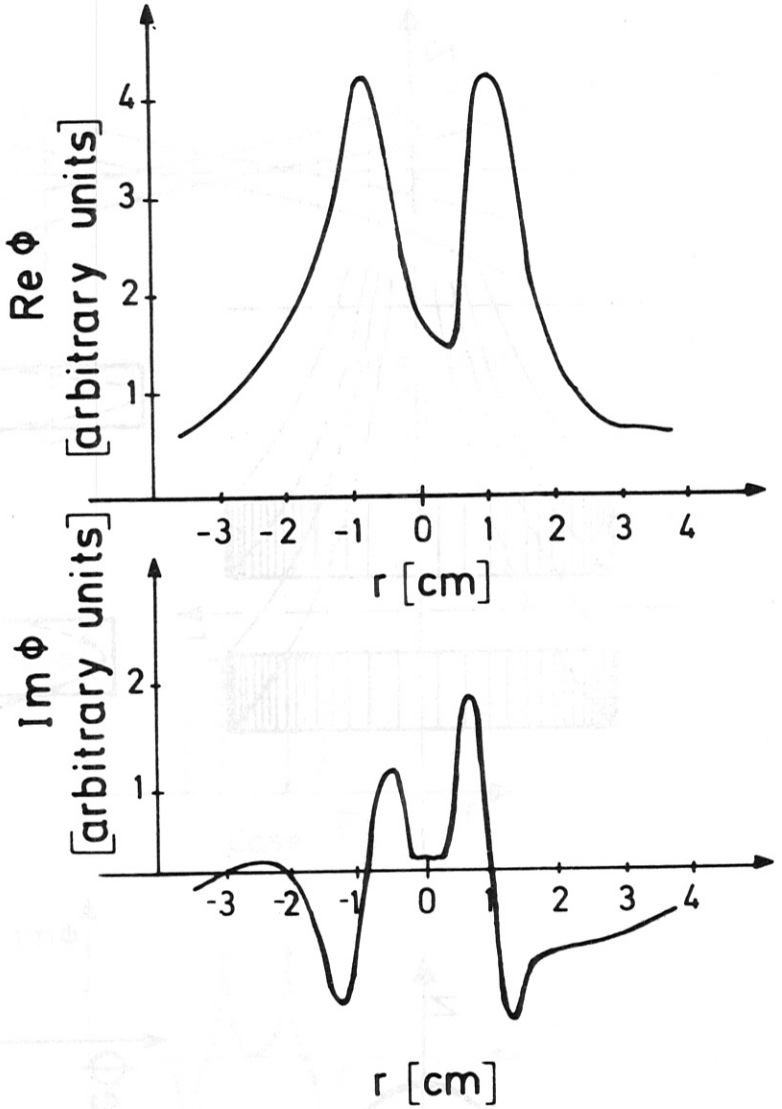
Re φ
[arbitrary units]
4
3
2
1
-3 -2 -1 0 1 2 3 4
r [cm]
Im φ
[arbitrary units]
2
1
-3 -2 -1 0 1 2 3 4
r [cm]

Fig.5a

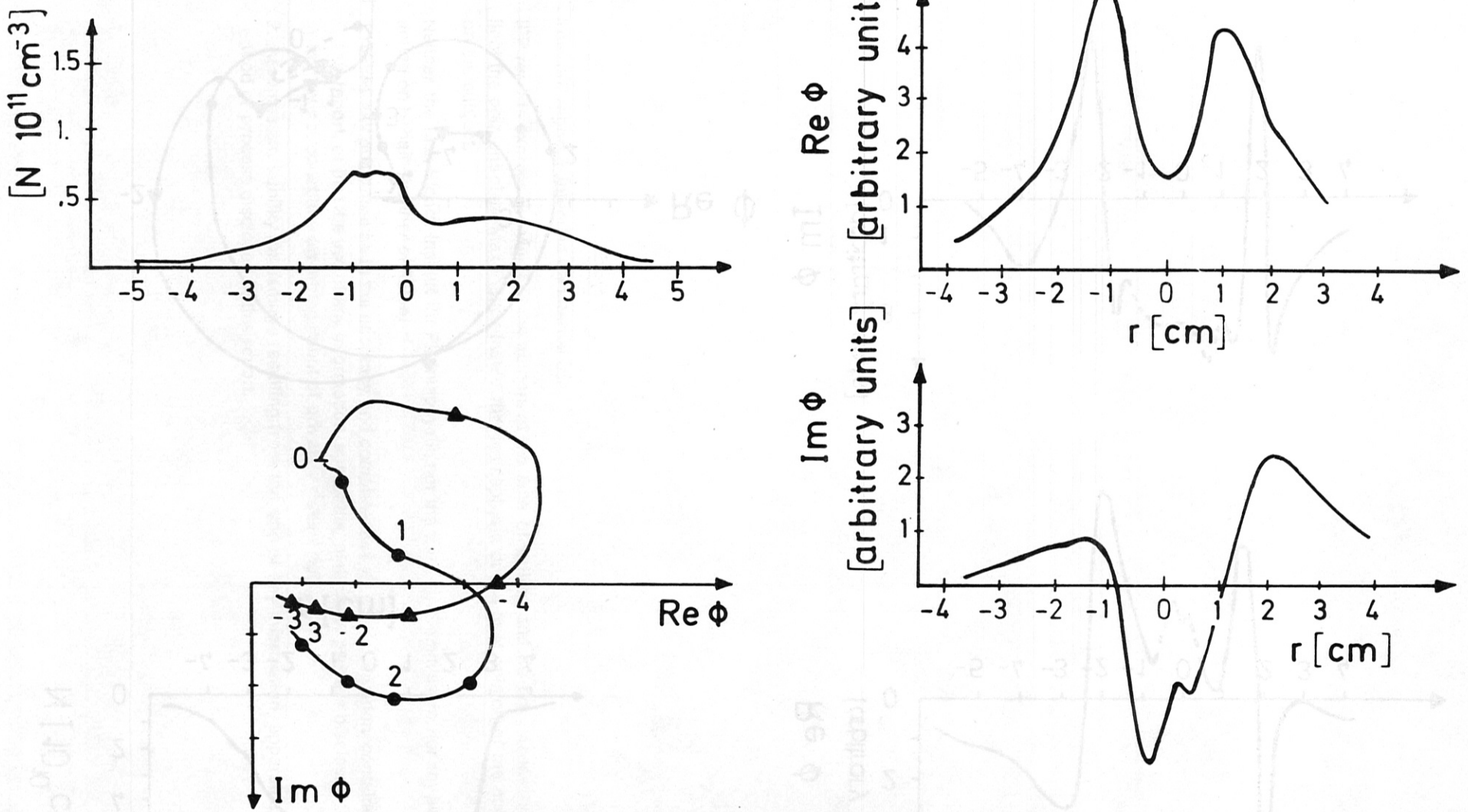
[N 10^11 cm^-3]
1.5
1.
.5
-5 -4 -3 -2 -1 0 1 2 3 4 5
0
1
2
3
-2
-3
-4
Re Φ
Im Φ
Re Φ [arbitrary units]
4
3
2
1
-4 -3 -2 -1 0 1 2 3 4
r [cm]
Im Φ [arbitrary units]
3
2
1
-4 -3 -2 -1 0 1 2 3 4
r [cm]

Fig. 5b

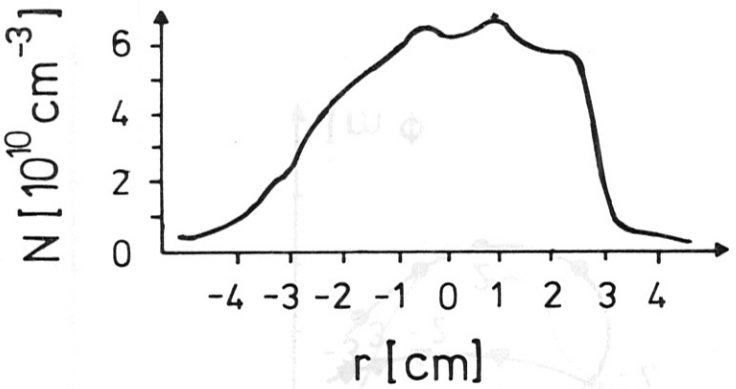
N [10^10 cm^-3]
6
4
2
0
-4 -3 -2 -1 0 1 2 3 4
r [cm]

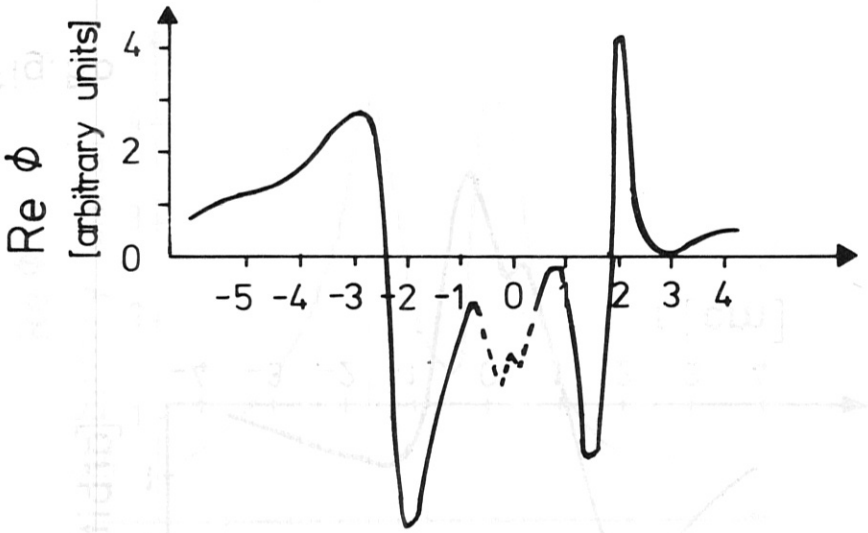
Re φ
[arbitrary units]
4
2
0
-5 -4 -3 -2 -1 0 1 2 3 4

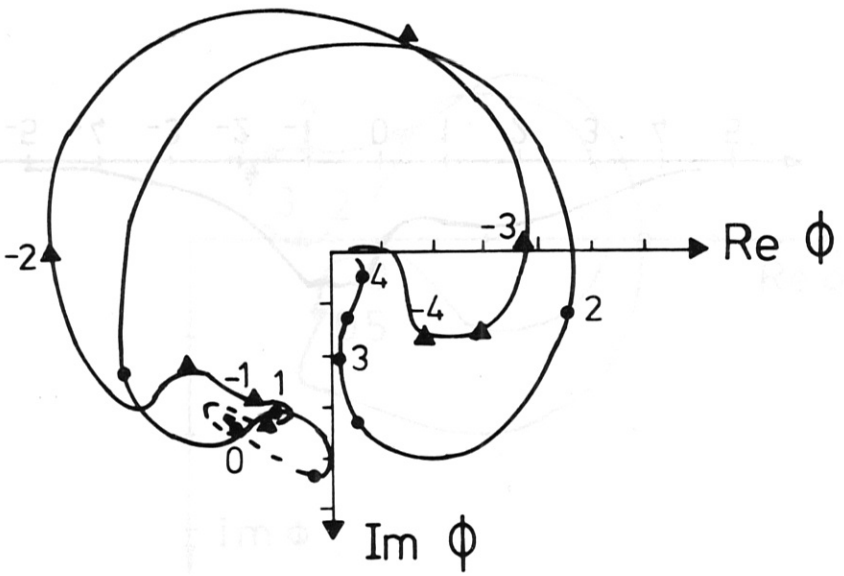
Re φ
Im φ
-2
-3
-4
2
3
4
-1
1
0

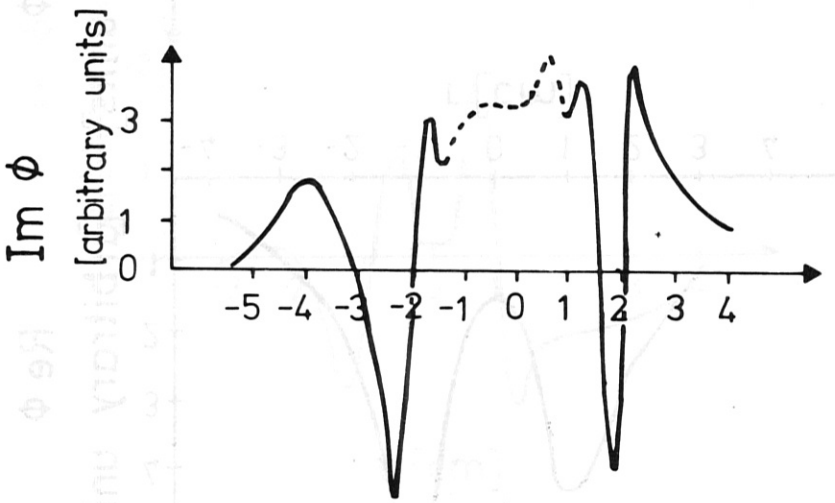
Im φ
[arbitrary units]
3
1
0
-5 -4 -3 -2 -1 0 1 2 3 4

Fig. 6